Available online at www.sciencedirect.com
ScienceDirect
Journal of Ethnopharmacology 112 (2007) 557–567
Journal of ETHNO-PHARMACOLOGY
www.elsevier.com/locate/jethpharm

Growth inhibitory and apoptosis inducing effect of *Perilla frutescens* extract on human hepatoma HepG2 cells

Chih-Sheng Lin [a,*], Chao-Lin Kuo [b], Jui-Ping Wang [a], Ju-Sang Cheng [a], Zheng-Wen Huang [a], Chi-Fei Chen [a]

[a] *Department of Biological Science and Technology, National Chiao Tung University, 75 Po-Ai Street, Hsinchu 30050, Taiwan*
[b] *School of Chinese Medicine Resources, China Medical University, Taichung 40402, Taiwan*

Received 21 September 2006; received in revised form 29 March 2007; accepted 1 May 2007
Available online 10 May 2007

Abstract

Perilla frutescens (L.) Britt. (Lamiaceae) has traditionally been used to treat diseases, including tumors, but the antitumorigenesis mechanism is unclear. We evaluated the effects of *Perilla frutescens* leaf extract (PLE) on proliferation and apoptosis inducing in human hepatoma HepG2 cells using a cell proliferation assay, flow cytometry, and cDNA microarrays. Gene expression and apoptosis were also assessed in HepG2 cells treated with a major constituent of PLE, rosmarinic acid (RosA). In the PLE-treated HepG2 cells, antiproliferative activity (105 μg/mL) were observed, flow cytometry revealed significant apoptosis, and microarray data indicated that the expression of a lot apoptosis-related genes were regulated in a time-dependent manner. Compared with PLE, RosA (10 μg/mL; a dose equivalent to 105 μg/mL of PLE) was less effective in increasing the expression of apoptosis-related genes and apoptosis inducing in HepG2 cells. Thus, additional PLE constituents may influence apoptosis in HepG2 cells. The results of our study suggest that the PLE should be further investigated as a promising to treat hepatocellular carcinoma.

Keywords: *Perilla frutescens*; Rosmarinic acid; cDNA microarray; Apoptosis; Hepatocellular carcinoma

1. Introduction

The leaves of *Perilla frutescens* (L.) Britt. (Lamiaceae) (*Perilla frutescens*), a traditional Chinese medicinal herb, have been used in the Orient for centuries to treat various conditions including depression (Takeda et al., 2002), infection (Kawahata et al., 2002), inflammation (Ueda et al., 2002; Banno et al., 2004), and allergies (Ueda et al., 2002; Makino et al., 2003; Takano et al., 2004). Several studies have also suggested that extract of *Perilla frutescens* is useful in antitumor growth in a murine skin model *in vivo* (Ueda et al., 2003; Banno et al., 2004; Osakabe et al., 2004). *In vitro* studies have reported that *Perilla frutescens* components, rosmarinic acid (RosA) and luteolin, can induce apoptosis in a variety of cancer cell lines (Hur et al., 2004; Kolettas et al., 2006; Selvendiran et al., 2006; Lim do et al., 2007). However, the mechanism of the antitumorigenesis effects of whole *Perilla frutescens* leaf extract (PLE) remains unclear.

Microarrays have become an important technology for identifying simultaneous and rapid changes in the expression of large numbers of genes. The technology has been adopted to investigate change in gene expression profiles as the results may help define the underlying antitumorigenesis properties of medicinal herb extracts (Yang et al., 2004; Kang et al., 2005; Hsieh and Wu, 2006; Huang et al., 2006). Therefore, a high-density cDNA microarray was used to differentiate gene expression in human hepatoma HepG2 cells in response to PLE treatment in the present study. We demonstrated that apoptosis induction in the HepG2 cells treated with PLE, which is related to the regulation of genes involving in apoptosis signaling pathways. To elucidate the active constituent in the PLE, we also compared the effects of PLE with purified RosA in the regulation of apoptosis-related gene expression.

* Corresponding author. Tel.: +886 3 5131338; fax: +886 3 5729288.
E-mail address: lincs@mail.nctu.edu.tw (C.-S. Lin).

0378-8741/$ – see front matter © 2007 Elsevier Ireland Ltd. All rights reserved.
doi:10.1016/j.jep.2007.05.008

2. Materials and methods

2.1. Preparation of PLE

Dried leaves of a green type of *Perilla frutescens* (L.) Britt. (Lamiaceae) were purchased from a Chinese herbal store in Hsinchu, Taiwan, and was authenticated by Prof. Kuo Chao-Lin at the School of Chinese Medicine Resources, China Medical University, Taiwan. A voucher specimen (CMU PF 0611) has been deposited at the China Medical University. The dried-herb product (50 g) was chopped, boiled in 1 L of distilled water for 1 h, and filtered through a membrane filter with a 0.45 μm pore size (Millipore, Bedford, MA). The supernatant was lyophilized, and the resulting powder, which corresponded to approximately 10% of the original weight of the dry leaves, was used in future studies.

2.2. High performance liquid chromatography assay

The concentrations of polyphenolic substances in the PLE, including RosA and caffeic acid, were determined by high performance liquid chromatography (HPLC). The HPLC system consisted of a Waters 717 Plus (Waters, Milford, CA) plus autosampler and a Waters 2996-photodiode array detector. A reverse-phase C_{18} column (250 mm × 4.6 mm i.d., 5 μm; ThermoQuest, Austin, TX) was used. The mobile phase was solvent A (methanol–water–formic acid, 14:85.2:0.8, v/v/v) and solvent B (methanol–water, 65:35, v/v). The gradient mode of HPLC was performed under the following conditions: 0% B for 5 min followed by a 30–45% linear gradient of A in B for 30 min (Fig. 1). The flow rate was 1 mL/min, and the optical density of effluent was monitored at 320 nm. Commercial RosA was obtained from Extrasynthase (Genay, France), and caffeic acid was purchased from Sigma (St. Louis, MO).

2.3. Cell culture

Human hepatoma cell line (HepG2) and normal liver cell line (WRL) were obtained from the American Type Culture Collection (ATCC). The cells were maintained in Minimum Essential Medium (MEM) (GIBCO Invitrogen, Grand Island, NY) supplemented with 1 mM sodium pyruvate and 10% fetal bovine serum (GIBCO Invitrogen) and cultured at 37 °C in a humidified atmosphere of 5% CO_2.

2.4. 3-(4,5-dimethylthiazol-2-yl)-2,5-diphenyl tetrazolium bromide assay

Inhibition of cell growth was determined by 3-(4,5-dimethylthiazol-2-yl)-2,5-diphenyl tetrazolium bromide (MTT) assay. HepG2 cells were seeded in 96-well plates (1×10^4 cells/well), each well containing 100 μL of fresh medium. The cells were cultured at 37 °C for 24 h. The PLE was then added to the wells in doses of 0, 50, 100, 200, 300, 400, and 500 μg/mL. After 24, 48, and 72 h of PLE treatment, the cells were treated with 10 μL of MTT (15 mg/mL in PBS, pH 7.4; Sigma) and were incubated for another 4 h. The medium was aspirated and replaced with DMSO, and the plate was agitated. The plate was read on a Bio-Rad 550 plate reader (Bio-Rad, Hercules, CA) at 570 nm with a 630 nm reference to eliminate the effect of cell debris. The PBS-treated cells, which did not receive PLE treatment, were used as a control for 0% growth inhibition.

2.5. Flow cytometry analysis

The Annexin V Apoptosis kit (Gene Research Lab, Taipei, Taiwan) was used to assay apoptosis according to the manufacturer's instructions. HepG2 cells were seeded in 6-well plates (2×10^5 cells/well) and incubated with 105 μg/mL of PLE for 0, 24, 48, and 72 h. To collect the cells, 2 mL of trypsin-EDTA solution (0.05% trypsin and 0.53 mM EDTA; GIBCO Invitrogen) was added for another 5 min at 37 °C. After centrifuging at 400 × *g* for 5 min, the cell pellets were obtained. The cell pellets were washed twice with cold Hanks' Balanced Salt Solution (HBSS; GIBCO Invitrogen) and then resuspended in Solution A at 1×10^6 cells/mL (Solutions A, B, and C were obtained from the Annexin V Apoptosis kit). The supernatant was discarded after centrifuging at 200 × *g* for 5 min at 25 °C. The cell pellets were suspended by adding 100 μL of Solution A, 2 μL of Solution B, and 5 μL of Solution C. The cells were gently agitated

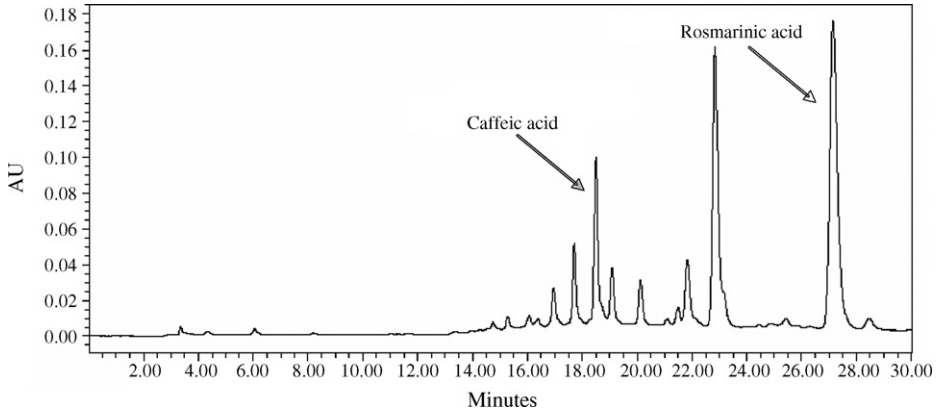

Fig. 1. HPLC chromatogram of *Perilla frutescens* leaf extract (PLE). Peaks of rosmarinic acid (RosA) and caffeic acid of PLE in the HPLC profile were identified by comparison with the retention times and UV spectra of standard compounds.

and incubated at 25 °C for 15 min. Finally, 400 μL of Solution A was added to each tube, and the cells were analyzed by flow cytometry (CyFlow®SL, Partec, Germany).

2.6. RNA isolation

HepG2 cells were cultured for 24, 48, and 72 h with 105 μg/mL of PLE or PBS. Total cellular RNA of each treatment was extracted using Trizol Reagent (GIBCO Invitrogen), and mRNA was purified by using the Oligotex mRNA Midi kit (Qiagen, Hilden, Germany) according to the manufacturer's instructions and previously reported procedures (Lin and Hsu, 2005). Examination and quantification of the purified mRNA was performed by determining A_{260}/A_{280} using a spectrophotometer and agarose gel electrophoresis.

2.7. Preparation of fluorescently labeled cDNA

Fluorescently labeled cDNA derived from mRNA was prepared by direct incorporation of fluorescent nucleotide analogs during a first-strand reverse transcription (RT) reaction. Each 40-μL labeling reaction consisted of 200 ng mRNA, 2 mM oligo-dT primer (GIBCO Invitrogen), 0.5 mM each of dATP, dCTP and dGTP, 0.2 mM dTTP, 10 mM DTT, 200 U/μL of Superscript III reverse transcriptase (Stratagene, La Jolla, CA) in RT buffer provided by the manufacturer, and 2 nmol of either cyanine-3 dUTP (Cy3) for the PBS-treated cells or cyanine-5 dUTP (Cy5) for the PLE-treated cells (Amersham Pharmacia Biotech, Piscataway, NJ). The mRNA and primers were preheated to 70 °C for 5 min and snap-cooled in ice water before adding the remaining reaction components. RT reaction proceeded for 10 min at 25 °C followed by 2 h at 42 °C. After RT reaction, the cDNA labeled with Cy3 and Cy5 were mixed and purified using Microcon YM-30 membrane cartridges (Millipore). Twenty μL of labeled cDNAs were recovered and added to 20 μL of 2× hybridization buffer (50% formamide, 10× SSC, 0.2% SDS, and 0.2 mg/mL of sheared salmon sperm DNA) and maintained at 95 °C for 3 min before being pelleted for 2 min in a tabletop centrifuge and kept at room temperature for an additional 20 min.

2.8. cDNA microarray hybridization

The procedure of competitive hybridization of cDNA microarray was performed as described (Lin and Hsu, 2005). A 24 mm × 50 mm cover slip was used to gently cover the

Table 1
The primers used in this study for semiquantitative RT-PCR assay

Gene (GenBank accession no.)	Primer[a]	Sequence (5′–3′)	PCR cycle	Amplified size (bp)[b]
Caspase-8 (NM_001228)	F	GGA GAC AAG GGC ATC ATC	30	329
	R	TGG CAA AGT GAC TGG ATG TAC		
NFκBIA (NM_020529)	F	AGC GTG GGA GTC CTG AC	28	433
	R	GCT CGT CCT CTG TGA ACT C		
TNFSF9 (NM_003811)	F	CCA AAA TGT TCT GCT GAT CG	26	414
	R	AAG ACT GTG GCG CCC TG		
Jun (NM_002228)	F	AAC CTC AGC AAC TTC AAC CC	28	320
	R	GCG ATT CTC TCC AGC TTC C		
Jun-B (NM_002229)	F	CTG CAC AAG ATG AAC CAC G	28	473
	R	AGC GTC TTC ACC TTG TCC T		
Fos-B (NM_006732)	F	GGA ACG AAA TAA ACT AGC AGC	28	489
	R	TGG TCA CTG CCG CTG GT		
Bax (AY217036)	F	ATG CGT CCA CCA AGA AGC TG	28	437
	R	CCA CTG TGA CCT GCT CCA GAA		
Bcl-2 (BC027258)	F	CAC CTG TGG TCC ACC TGA C	34	290
	R	GTG CAG GTG CCG GTT CA		
GAPDH (NM_002046)	F	GCC AAA AGG GTC ATC ATC TC	28	622
	R	TGT TGC TGT AGC CAA ATT CG		

Caspase-8, caspase 8-apoptosis-related cysteine protease; NFκBIA, nuclear factor of kappa light polypeptide gene enhancer in B-cells inhibitor-alpha; TNFSF9, tumor necrosis factor ligand superfamily-member 9; Jun, v-jun sarcoma virus 17 oncogene; Jun-B, oncogene JUN-B; Fos-B, FBJ murine osteosarcoma viral oncogene homolog B; Bax, pro-apoptotic Bcl-2 associated protein X; Bcl-2, B-cell CLL/lymphoma 2; GAPDH, glyceraldehyde-3-phosphate dehydrogenase.

[a] F, forward primer; R, reverse primer.

[b] Including the sequences of F and R primers.

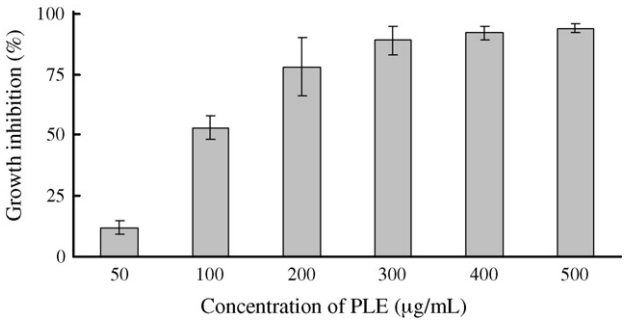

Fig. 2. Dose-dependent inhibition of growth on human hepatoma HepG2 cells by PLE treatment. The cells (1×10^4 cells/well) were seeded in 96-well plates for 24 h and then treated with 0 (PBS), 50, 100, 200, 300, 400, and 500 μg/mL of PLE. After treatment for another 72 h, cell viability was measured by MTT assay. PBS-treated cells served as a control (i.e., 0% growth inhibition). Each value is expressed as a mean ± S.D. of six independent determinations.

microarray that contains 7680 sequences of cDNA and expressed sequence tags (ESTs) (UniversoChip 8K-1, AsiaBioinnovations Co., Newark, CA). Arrays were pre-hybridized for 2 h at 42 °C in hybridization buffer. The fluorescently labeled cDNAs were added, and hybridization was carried out in a humidified slide chamber for 12 h at 42 °C. After hybridization, the arrays were washed twice for 15 min in 2× SSC/0.1% SDS at room temperature and again washed twice for 15 min in 0.1× SSC/0.1% SDS at 42 °C. The slide was scanned at 532 nm (for Cy3) and 635 nm (for Cy5) using the Axon GenePix 4000B microarray scanner (Axon Instruments Inc., Union City, CA). The microarray images were analyzed using Axon GenPix Pro-4.0 software (Axon Instruments Inc.).

2.9. Cluster analysis

The GeneCluster software (http://www.genome.wi.mit.edu) was used to generate normalized intensity values for each gene in each microarray by using the overall mean intensity of the array as the normalization standard. These values were averaged across each experimental group. The averages of ratios for the same gene in the groups were then calculated, representing the relative expression levels of a certain gene under specific conditions. Average linkage hierarchical cluster analysis was performed to organize gene expression data. The data were processed using the software TreeView (http://www.genome.wi.mit.edu), and the intensities associated with the expression of various genes were compared (Campos et al., 2003).

2.10. Reverse transcription-polymerase chain reaction measurement of mRNA expression

The semi-quantitative RT-polymerase chain reaction (RT-PCR) method was adapted to verify hybridization data derived from the cDNA microarray. Nine sets of PCR primers, including forward and reverse primers, were designed to detect gene expression (Table 1). Primer sequences were designed using Primer Express software (Applied Biosystems, Foster, CA) and synthesized by Applied Biosystems (Applied Biosystems). As an internal control, the gene encoding glyceraldehyde-3-phosphate dehydrogenase (GAPDH) was included for semi-quantitative RT-PCR analysis.

For cDNA synthesis, 3 μg of total cellular RNA was supplemented in a total reaction volume of 20 μL with 5× RT reaction buffer (250 mM Tris–HCl, pH 8.3, 375 mM KCl, 15 mM $MgCl_2$), 0.5 mM dNTPs, 2.5 μM oligo-dT, 40 U/μL RNase inhibitor (RNaseOUT; GIBCO Invitrogen), and 200 U/μL of Superscript III reverse transcriptase. After incubation for 60 min at 50 °C, the mixture was incubated for 15 min at 70 °C to denature the products. The mixture was then chilled on ice and applied for PCR. PCR reactions contained 3 μL of cDNA, 1 μL of each primer (10 μM), 5 μL of 10× PCR buffer (100 mM Tris–HCl, pH 9.0, 15 mM MgCl, 500 mM KCl, 1% (v/v) Triton X-100, 0.1% (w/v) gelatin), 2 μL of 10 mM dNTPs, 1 μL of 0.5 U Super Taq DNA polymerase (HT Biotechnology Ltd., Cambridge, England), and 38 μL of distilled water in a total volume of 50 μL. Thermal cycler (MiniCycler; MJ Research, Waltham, MA) conditions were as follows: 94 °C for 5 min, followed by 26–34 cycles of denaturation at 94 °C for 30 s, annealing at 55 °C for 30 s, and elongation at 72 °C for 45 s, and finally 72 °C for 3 min. The resulting PCR products were visualized on 2% agarose gels stained with ethidium bromide under UV light (Bio-Rad), and the band intensity was quantified using densitometric analysis by Scion image (Scion, Frederick, MD). The relative mRNA expression of the following genes was calculated as ratios to GAPDH expression: caspase 8-apoptosis-related cysteine protease (Caspase-8), nuclear factor of kappa light polypeptide gene enhancer in B cells inhibitor-alpha (NFκBIA), tumor necrosis factor ligand superfamily-member 9 (TNFSF9), v-jun sarcoma virus 17 oncogene (Jun), oncogene JUN-B (Jun-B), FBJ murine osteosarcoma viral oncogene homolog B (Fos-B), pro-apoptotic Bcl-2 associated protein X (Bax) and B cell CLL/lymphoma 2 (Bcl-2).

2.11. Effects of RosA in HepG2 cells

HepG2 cells were treated with commercially available RosA at concentrations of 5 and 10 μg/mL, which are dose equivalents to 52.5 and 105 μg of the PLE, respectively. The cells were applied to MTT and flow cytometry analyses after 72 h of the treatment, and the total cellular RNA were also prepared for RT-PCR assay to measure the mRNA expression of Caspase-8, NFκBIA, TNFSF9, Jun, Jun-B, Fos-B, Bax, Bcl-2 and GAPDH.

2.12. Statistical analysis

All data are presented as the mean ± standard deviation (S.D.). Differences between groups were evaluated by a two-tailed Student's *t*-test. Mean values were considered to be statistically significant at p value < 0.05.

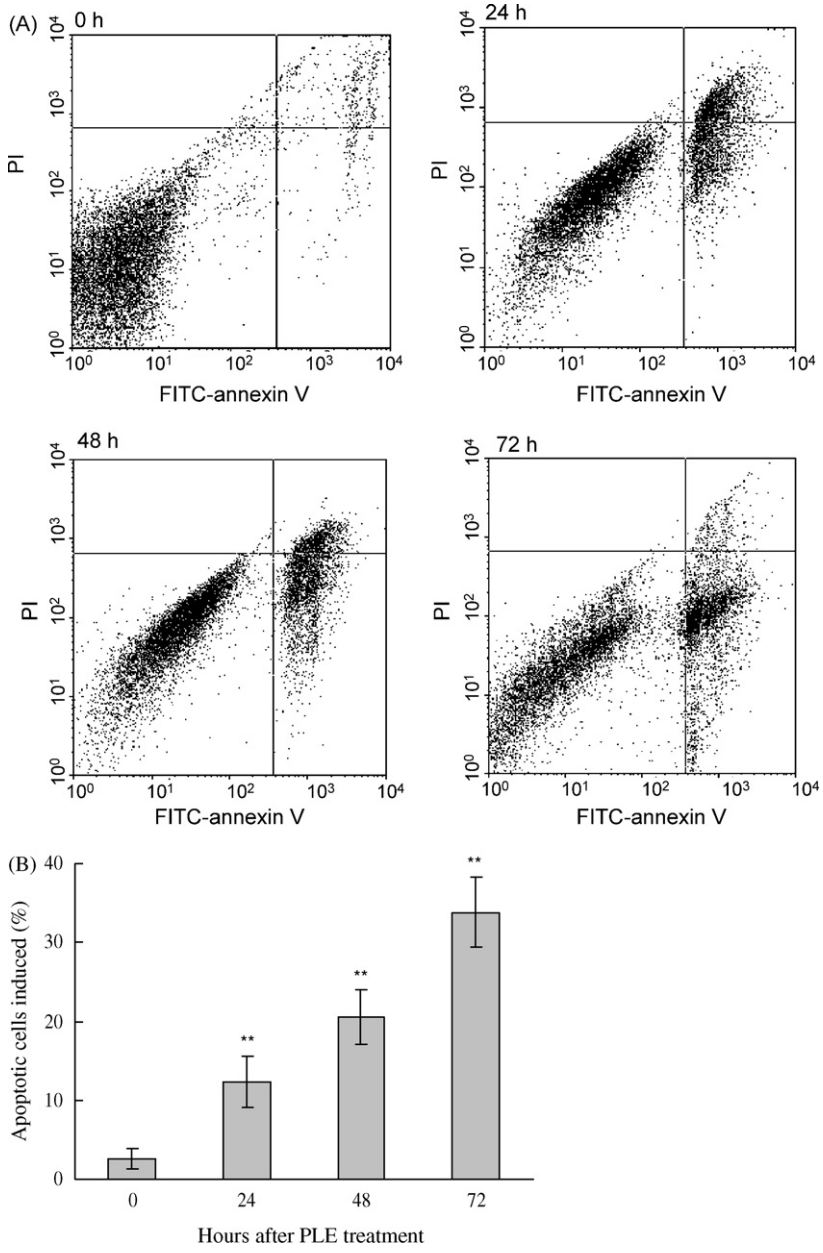

Fig. 3. Contour diagram of FITC-annexin V/PI flow cytometry of HepG2 cells treated with 105 μg/mL of PLE for 0, 24, 48, and 72 h. The lower left quadrant in each panel represents the viable cells, which excluded PI and are negative for FITC-annexin V binding. The upper right quadrants contain non-viable, necrotic cells, which are positive for FITC-annexin V binding and for PI uptake. The lower right quadrants contain the apoptotic cells, FITC-annexin V-positive and PI negative, indicating cytoplasmic membrane integrity and apoptosis. One representative experiment of the three flow cytometric determinations is shown (A). After 24, 48, and 72 h of exposure to 105 μg/mL of PLE, the apoptotic cell percentages were 12.3 ± 3.2%, 20.5 ± 3.4% and 33.8 ± 4.5% (mean ± S.D., $n = 3$ for each time point), respectively (B). $^{**}p < 0.01$ vs. control (0 h of treatment).

3. Results

3.1. HPLC analysis

Biologically active components, such as luteolin, caffeic acid, triterpene acid and RosA, have been identified from *Perilla frutescens* (Peng et al., 2005). Therefore, in this study, commercially available RosA and caffeic acid were used as standard compounds for our HPLC analysis (i.e., with respect to UV spectra and retention time) (Fig. 1). We found that RosA is a major component in the PLE and accounted for approximately 9.4% of the total PLE (weight of RosA/dried weight of PLE).

3.2. MTT analysis

The MTT assay was used to evaluate whether PLE inhibited the growth of hepatoma HepG2 cells over 72 h of treatments (Fig. 2). The IC_{50} (50% of growth inhibition) was calculated to be 105 ± 8 μg/mL. Therefore, 105 μg/mL of PLE was used in apoptosis assay and in cDNA microarray experiments. Growth inhibition in WRL cells following PLE treatment was also

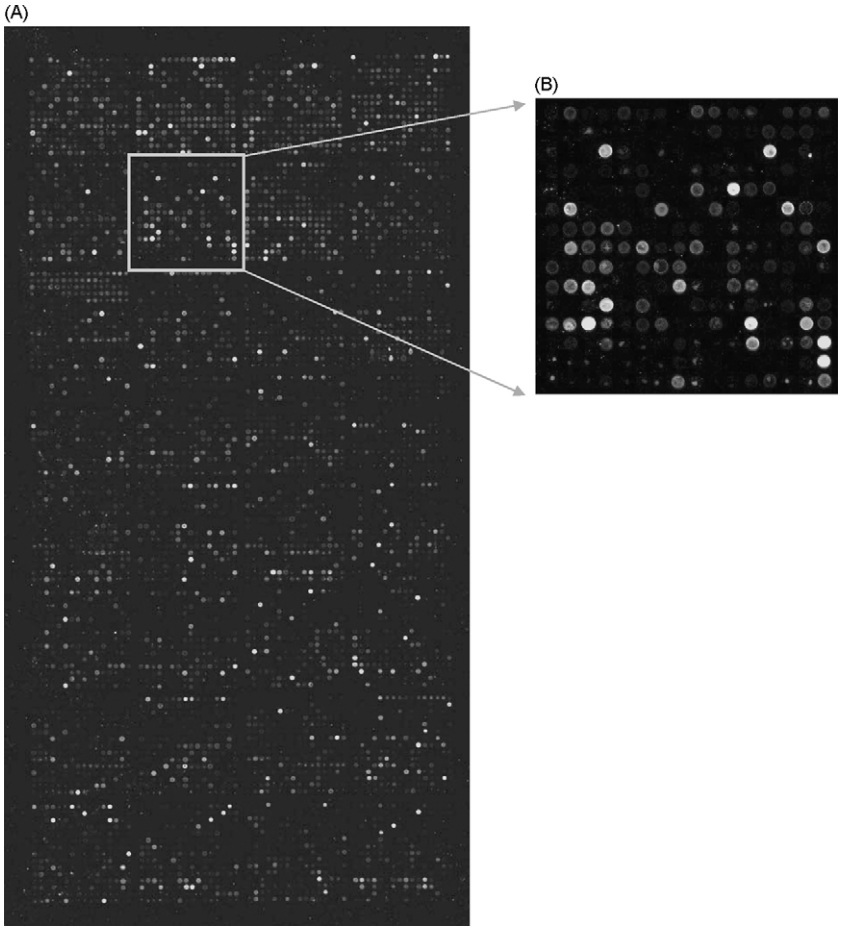

Fig. 4. One of cDNA microarray images after competitive hybridization and fluorescence scanning (A) and the partial images in the microarray (B). Total cellular RNAs of HepG2 cells treated with PLE and with PBS for 72 h were labeled with cyanine 5-dUTP (Cy5) and cyanine 3-dUTP (Cy3) by reverse transcription, respectively. The labeled cDNAs were applied on the cDNA microarray for competitive hybridization and scanned by the Axon GenePix 4000B microarray scanner.

evaluated. However, WRL cells were much less susceptible than HepG2 cells to the cytotoxic effects of PLE, in that growth inhibition of WRL cells reached only $4.2 \pm 2.5\%$ at 500 μg/mL PLE, and the IC_{50} was calculated to be >2 mg/mL.

3.3. Apoptosis assay

Fig. 3A shows the annexin V-FITC/PI analysis of HepG2 cells cultured with 105 μg/mL of PLE for 0, 24, 48, and 72 h. Apoptotic cells appeared in the annexin V^+/PI^- fraction, whereas, cells damaged by scraping appeared in the annexin V^-/PI^+ fraction, and late apoptosis or necrotic cells were evident in the annexin V^+/PI^+ fraction. The three independent measurements made after 24, 48, and 72 h of exposure to 105 μg/mL of PLE revealed that the percentages of apoptotic cells (annexin V^+/PI^- fraction) were $12.3 \pm 3.2\%$, $20.5 \pm 3.4\%$, and $33.8 \pm 4.5\%$, respectively (Fig. 3B).

3.4. cDNA microarray analysis

Duplicate analyses of the cDNA microarray were made for each treatment of HepG2 cells with 105 μg/mL of PLE for 24, 48, and 72 h. After hybridization, an average of 4800/7680 sequences (62.5%) had signal intensities that were greater (twofold) than background in both Cy3 and Cy5 channels (Fig. 4). In this study, a difference of at least twofold in the normalized intensity ratio (Cy5/Cy3 or Cy3/Cy5) was regarded as significant. The treatment of HepG2 cells with 105 μg/mL of PLE for 24 h up-regulated 62 genes, whereas, 319 genes and 609 genes were up-regulated in HepG2 cells treated for 48 and 72 h, respectively. The genes whose differential up-regulation was induced by PLE are involved in many apoptosis-related functions (data not shown). Thirty-three apoptosis genes expressed in the HepG2 cells treated with PLE for 72 h had signal intensities that were twofold greater than the signal intensities in PBS-treated control cells (Table 2).

Furthermore, the clustering results indicated that some up-regulated genes associated with apoptosis pathways function in a time-dependent manner. For example, one of the clusters showed that apoptosis-related genes, including Caspase-8, Jun-B, TNFSF9 and Fos-B, had time-dependent up-regulated expression (Fig. 5).

Fig. 6 shows the microarray expression profiles of eight apoptosis-related genes (Caspase-8, NFκBIA, TNFSF9, Jun, Jun-B, Fos-B, Bax, and Bcl-2) as they correspond to duration of PLE exposure. In HepG2 cells treated with PLE, the gene

Table 2
Up-regulated genes related to apoptosis induction in the HepG2 cells treated with PLE at concentration of 105 μg/mL for 72 h

GenBank accession no.	Gene name	Gene symbol	Ratio[a]
NM_014002	Inhibitor of kappa light polypeptide gene enhancer in B-cells-kinase epsilon	IKBKE	3.41
NM_002791	Proteasome (prosome-macropain) subunit-alpha type-6	PSMA6	4.44
NM_003478	Cullin 5	CUL5	6.32
NM_006509	V-rel reticuloendotheliosis viral oncogene homolog B-nuclear factor of kappa light polypeptide gene enhancer in B-cells 3 (avian)	RELB	2.15
NM_003682	MAP-kinase activating death domain	MADD	3.64
NM_000021	Presenilin 1 (Alzheimer disease 3)	PSEN1	2.77
NM_031449	Hypothetical protein DKFZp761I2123	DKFZp761I2123	5.18
NM_002859	Paxillin	PXN	4.33
NM_001228	Caspase 8-apoptosis-related cysteine protease	CASP8	3.02
NM_003969	Ubiquitin-conjugating enzyme E2M (UBC12 homolog-yeast)	UBE2M	2.41
NM_002808	Proteasome (prosome-macropain) 26S subunit-non-ATPase-2	PSMD2	3.73
NM_002462	Myxovirus (influenza virus) resistance 1-interferon-inducible protein p78 (mouse)	MX1	2.55
NM_014330	Protein phosphatase 1-regulatory (inhibitor) subunit 15A	PPP1R15A	4.12
NM_003745	Suppressor of cytokine signaling 1	SOCS1	3.34
NM_001681	ATPase-Ca^{2+} transporting- cardiac muscle-slow twitch 2	ATP2A2	5.42
NM_003811	Tumor necrosis factor (ligand) superfamily-member 9	TNFSF9	4.86
NM_001001716	Nuclear factor of kappa light polypeptide gene enhancer in B-cells inhibitor-beta	NFκBIB	2.32
NM_004226	Serine/threonine kinase 17b (apoptosis-inducing)	STK17B	5.29
NM_006595	Apoptosis inhibitor 5	API5	3.78
NM_005339	Huntingtin interacting protein 2	HIP2	2.46
NM_000061	Bruton agammaglobulinemia tyrosine kinase	BTK	4.08
NM_004330	BCL2/adenovirus E1B 19 kDa interacting protein 2	BNIP2	2.47
NM_014456	Programmed cell death 4 (neoplastic transformation inhibitor)	PDCD4	3.97
NM_001949	E2F transcription factor 3	E2F3	3.39
NM_002229	Jun B proto-oncogene	JUNB	5.49
AF083340	Double-stranded RNA-binding zinc finger protein JAZ	JAZ	4.74
NM_003151	Signal transducer and activator of transcription 4	STAT4	3.99
NM_006499	Lectin-galactoside-binding-soluble-8 (galectin 8)	LGALS8	3.13
NM_006732	FBJ murine osteosarcoma viral oncogene homolog B	FOSB	7.64
NM_000484	Amyloid beta (A4) precursor protein (protease nexin-II-Alzheimer disease)	APP	2.47
NM_020529	Nuclear factor of kappa light polypeptide gene enhancer in B-cells inhibitor-alpha	NFκBIA	3.04
NM_000595	Lymphotoxin alpha (TNF superfamily-member 1)	LTA	2.98
NM_002228	V-jun sarcoma virus 17 oncogene homolog	JUN	4.94

[a] The rates were calculated by Cy5 intensity/Cy3 intensity, i.e. the expression level of individual mRNA in the HepG2 cells treated with 105 μg/ml of PLE for 72 h compared with that of the cells treated with PBS for 72 h. The ratio >twofold was considered significantly different and listed in this table.

expression profiles showed significant up-regulation of Caspase-8, NFκBIA, TNFSF9, Jun, Jun-B, Fos-B and Bax; however, down-regulation of Bcl-2.

3.5. Verification of differentially expressed genes by RT-PCR

To validate our cDNA microarray approach for identifying differentially transcribed genes, we performed semi-quantitative RT-PCR on the eight apoptosis-related genes and GAPDH (as a co-variant) at 0, 24, 48, and 72 h after PLE treatment (105 μg/mL) (Fig. 7A). Messenger RNA expression of Caspase-8, NFκBIA, TNFSF9, Jun, Jun-B, Fos-B and Bax was slightly induced at 24 h after PLE treatment and was significantly induced at 48 or 72 h. In contrast, Bcl-2 mRNA expression was significantly reduced at 48 and 72 h (Fig. 7B). The mRNA expression of the selected genes measured by semi-quantitative RT-PCR tended to be consistent with the relative expression measured by the cDNA microarray. The quantitative RT-PCR results confirm the microarray results, demonstrating that the microarray technique used in this study is accurate and reproducible.

3.6. Effects of RosA on apoptosis in HepG2 cells

HepG2 cells were treated with commercially available RosA at concentrations of 5 and 10 μg/mL, which are dose equivalents to 52.5 and 105 μg/mL of the PLE, respectively. After exposure to 10 μg/mL of RosA for 72 h, the percentage of growth inhibition and apoptotic HepG2 cells was $35.9 \pm 6.7\%$ and $22.1 \pm 3.8\%$, respectively. Both values were significantly larger than those in the cells treated with 5 μg/mL of RosA (Fig. 8). Following treatment with 10 μg/mL of RosA, semi-quantitative RT-PCR analysis of the eight selected apoptosis-related genes showed that Caspase-8, NFκBIA, TNFSF9 and Jun mRNA expression was significantly induced, and Bcl-2 mRNA expression was significantly reduced. With the exception of Caspase-8 and TNFSF9, changes in expression of the other

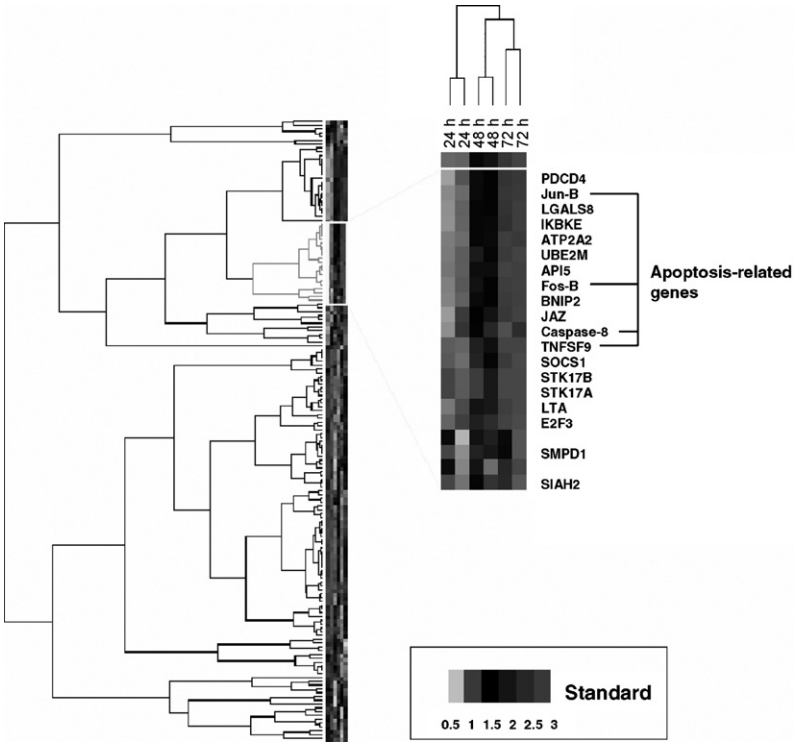

Fig. 5. Partial hierarchical cluster of gene expression profiles of HepG2 cells treated with PLE. The cluster was obtained using the Pearson correlation and complete linkage functions provided by GeneCluster software (http://www.genome.wi.mit.edu). Cluster analysis revealed the clustering of duplicate microarray data for 24, 48, and 72 h, respectively. Parts of the cluster that reveal time-dependent up-regulation of gene expression are presented. In this cluster, up-regulated expression was observed for the following genes associated with apoptosis: Jun-B, Fos-B, Caspase-8 and TNFSF9. The color indicates the log of the Cy5/Cy3 ratio, and the brightness increases with the magnitude of the ratio.

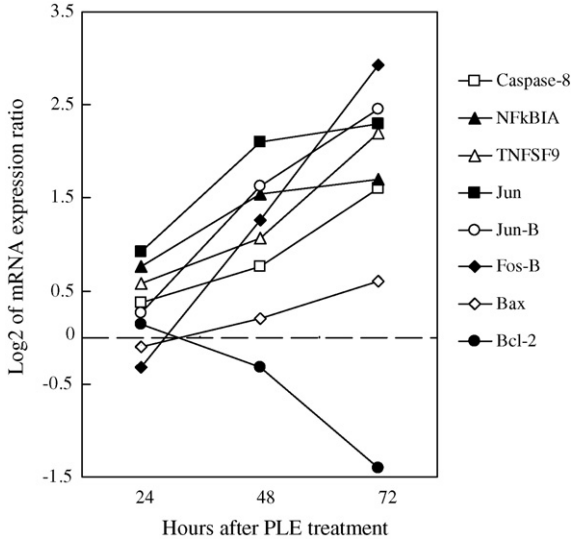

Fig. 6. Time-dependent changes of the expression of apoptosis-related genes in HepG2 cells treated with PLE. HepG2 cells were treated with 105 μg/mL of PLE for 24, 48, and 72 h. The mRNAs were then subjected to microarray hybridization. Each value indicates the mean of intensity ratios of Cy5 (treated with PLE)/Cy3 (treated with PBS, as a control) obtained from duplicate microarray results. The results are depicted as ratios of the fluorescence signal intensities from HepG2 cells exposed to PLE for the indicated times compared with the parallel PBS treatment. Log 2 of ratio values for Caspase-8, NFκBIA, TNFSF9, Jun, Jun-B, Fos-B, Bax, and Bcl-2 derived from microarray hybridization experiments were plotted with respect to the duration of PLE exposure.

apoptosis-related genes were not significant following treatment with 5 μg/mL of RosA (Fig. 7B).

4. Discussion

The results presented herein demonstrate that the PLE inhibits the growth of HepG2 cells in a dose-dependent manner. However, PLE did not significantly affect the growth of a normal liver cell line, confirming tumor-selective growth inhibition. PLE treatment of HepG2 cells increased apoptosis in a time-dependent manner, and increased mRNA expression from several genes that encode proteins related to apoptosis induction. These results demonstrate that PLE effectively induces apoptosis on human hepatoma HepG2 cells.

Apoptosis-inducing substances have been screened and used as antitumor agents *in vitro* (Kang et al., 2000; Kuo et al., 2000; Yoo et al., 2002), *in vivo* (Lee et al., 2006), and in clinical research (Davis et al., 2003; Kyprianou, 2003). The results of cDNA microarray and RT-PCR analyses in this study showed that expression of Caspase-8, NFκBIA, TNFSF9, Jun, Jun-B, Fos-B and Bax was up-regulated and expression of Bcl-2 was down-regulated in the PLE-treated HepG2 cells. This finding supports the idea that the antiproliferative effect(s) of PLE on HepG2 cells may reflect several changes in gene expression related to apoptosis induction. The activation of Caspase-8 by death receptor signals causes the cleavage of procaspase-3 (Stennicke et al., 1998). Caspase-8

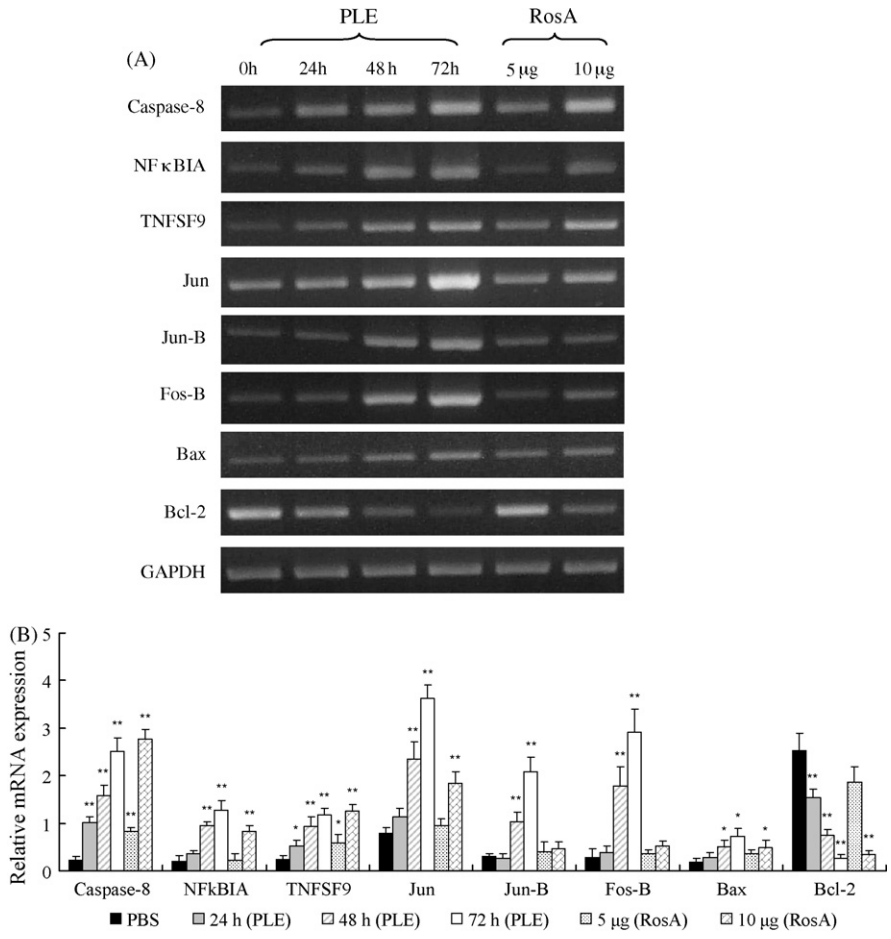

Fig. 7. Semi-quantitative RT-PCR assays of mRNA expression in HepG2 cells treated with PLE and RosA. HepG2 cells were treated with 105 μg/mL of PLE for 0, 24, 48, and 72 h and with 5 μg/mL and 10 μg/mL of RosA for 72 h. RT-PCR was used to detect the relative mRNA expression of Caspase-8 (329 bp), NFκBIA (433 bp), TNFSF9 (414 bp), Jun 320 bp), Jun-B (473 bp), Fos-B (489 bp), Bax (437 bp), Bcl-2 (290 bp), and GAPDH (622 bp, as an internal control). (A) One set of agarose gel images shows the detected RT-PCR products of the selected genes. (B) Histograms show the relative amount of each mRNA determined by densitometric analysis and normalized to the control (GAPDH), represented as relative mRNA expression. Data are presented as the mean ± S.D. of three experiments for each treatment. *$p < 0.05$, and **$p < 0.01$ vs. control (0 h of the treatment).

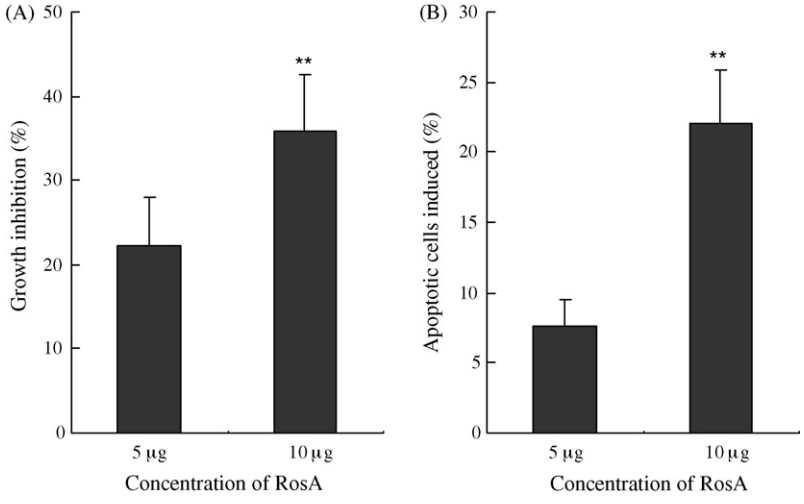

Fig. 8. Effects of growth inhibition and apoptosis induction in HepG2 cells treated with RosA. HepG2 cells were treated with commercially available RosA at concentrations of 5 and 10 μg/mL, which are dose equivalents to 52.5 and 105 μg of the PLE, respectively. The cells were applied to MTT (A) and flow cytometry (B) analyses after 72 h of the treatment. In the growth inhibition assay, PBS-treated cells served as a control (i.e., 0% growth inhibition). Each value is expressed as a mean ± S.D. of three independent determinations. **$p < 0.01$ vs. 5 μg/mL treatment.

also cleaves Bid, a pro-apoptotic member of the Bcl-2 family, and thereby stimulates release of mitochondrial cytochrome *c* into the cytosol in apoptosis (Luo et al., 1998). Members of the Bcl-2 family of intracellular proteins are the central regulators of caspase activation during apoptosis-related signaling, acting either as apoptotic agonists or antagonists (Cory and Adams, 2002). It has been reported that the prevention of apoptosis is associated with the up-regulation of Bcl-2 and the down-regulation of Bax (Cory and Adams, 2002; Wang et al., 2002; Chor et al., 2005). Because the antiapoptotic functions of Bcl-2 can be antagonized by pro-apoptotic proteins like Bax, the down-regulation of Bcl-2 and the up-regulation of Bax expression might explain its apoptotic inducing effect of PEL on HepG2.

HepG2 cells treated with PLE showed considerably higher expression of Jun-B and Fos-B mRNA; treatment with RosA, however, did not have the same effect. Moreover, HepG2 cells treated with either PLE or RosA had significantly up-regulated Caspase-8 expression and down-regulated Bcl-2 expression. These results suggest that RosA induces apoptosis in HepG2 cells via a mitochondrial pathway in which caspases and Bcl-2 act as apoptosis executioners rather than as inducers of apoptosis through a FOS/JUN-mediated mechanism. The up-regulated cytokine TNF-α, act through an autocrine pathway to induce cell growth arrest and apoptosis via NFκB activation (Kang et al., 2005; Lee et al., 2006). Similar result was observed in this study that TNFSF9 and NFKBIA were up-regulated in HepG2 cells treated with PLE and RosA.

The effects of RosA on apoptosis induction and changes in apoptosis-related gene expression were determined because RosA is a major polyphenolic compound in PLE. Osakabe et al. (2004) reported that an extract of *Perilla frutescens* containing 68% RosA causes a marked reduction of tumorigenesis in a murine two-stage skin model. RosA promotes apoptosis in human Jurkat T lymphoma cells via a mitochondrial pathway and suppressed by Bcl-2 in which caspases act as apoptosis executioners rather than as mitochondrial dysfunction inducers (Hur et al., 2004; Kolettas et al., 2006). The apoptosis of activated T cells from rheumatoid arthritis patients also can be induced by RosA treatment (Hur et al., 2007). Our result was confirmed by these reports that one of roles of RosA in apoptosis induction in HepG2 cells is via mitochondrial pathway. However, RosA was shown to inhibit adriamycin-induced apoptosis of a rat cardiac muscle cell line, H9c2, by inhibiting reactive oxygen species (Kim et al., 2005). It was also reported that RosA can inhibit sorbitol-induced apoptosis in human erythroleukemic cells (K562) (Salimei et al., 2007). In view of these relatively studies producing apparently conflicting observations on the antiapoptotic activity of RosA, the roles of RosA in cellular apoptosis remain to be clarified.

When HepG2 cells were treated with RosA, less effect of apoptosis induction and less changes of apoptosis-related gene expression were detected compared with HepG2 cells treated with PLE. This indicates that there are constituents in the herb other than RosA that are critical for its apoptosis inducing effect. However, significant changes in apoptosis-related gene expression, including expression from Caspase-8, NFκBIA, TNFSF9, Jun, Bax and Bcl-2, were also detected when the cells were treated with RosA. Despite the finding that isolated RosA has a weaker effect on apoptosis induction than PLE, there is little doubt that RosA is the main component responsible for the apoptosis-inducing effect of *Perilla frutescens* on HepG2 cells. As suggested by our results, we propose that additional *Perilla frutescens* components influence apoptosis induction in HepG2 cells. Besides RosA, triterpene acids (Banno et al., 2004) and luteolin (Ueda et al., 2003) extracted from *Perilla frutescens* leaves have been evaluated for their anticancer effects. Moreover, a methyl caffeate extracted from *Perilla frutescens* leaves also suppresses cancer cell growth by the inhibition of fos-jun-DNA complex formation (Lee et al., 2001). Therefore, the proliferative inhibitory and apoptosis inducing effects in HepG2 cells triggered by the biologically active components in *Perilla frutescens* remain to be explored.

In summary, the results of cDNA microarray analysis and RT-PCR assay identify the apoptosis-inducing genes responsible for the effects of PLE on HepG2 cells. The down-regulation of Bcl-2, up-regulation of caspase and other expressed genes involving in apoptotic signaling suggest that apoptosis induced by PLE may be mediated through multiple pathways. Various compounds in PLE, including RosA, may act to induce apoptosis in HepG2 cells. In fact, compounds such as RosA, luteolin, and triterpene acid isolated from *Perilla frutescens* have been reported to exhibit antitumor activity. However, the interactions between components in *Perilla frutescens* and other cellular factors that may induce apoptosis on human hepatoma HepG2 cells remain to be explored. This study is the first report that the extract of *Perilla frutescens* may lead to cancer cell death via the regulation of expressed genes related to cellular apoptosis. Whether the apoptosis inducing effect of PLE is a cell specific effect or not? It is possible that the genetic effects of PLE or RosA are different in different cell types. The experiments should be performed in other cancer cell lines before to conclude the PLE can be a promising of anticancer medicinal herb.

Acknowledgements

This work was supported by grants, NSC 91-2314-B-009-001-CC3 and NSC 92-2320-B-009-001, from the National Science Council of Taiwan. This work was also partially supported by the Taiwan Department of Education, under Grant of MOE 96W808 and ATU Programs.

References

Banno, N., Akihisa, T., Tokuda, H., Yasukawa, K., Higashihara, H., Ukiya, M., Watanabe, K., Kimura, Y., Hasegawa, J., Nishino, H., 2004. Triterpene acids from the leaves of *Perilla frutescens* and their anti-inflammatory and antitumor-promoting effects. Bioscience, Biotechnology, and Biochemistry 68, 85–90.

Campos, A.H., Zhao, Y., Pollman, M.J., Gibbons, G.H., 2003. DNA microarray profiling to identify angiotensin-responsive genes in vascular smooth muscle cells: potential mediators of vascular disease. Circulation Research 92, 111–118.

Chor, S.Y., Hui, A.Y., To, K.F., Chan, K.K., Go, Y.Y., Chan, H.L., Leung, W.K., Sung, J.J., 2005. Anti-proliferative and pro-apoptotic effects of herbal medicine on hepatic stellate cell. Journal of Ethnopharmacology 100, 180–186.

Cory, S., Adams, J.M., 2002. The Bcl2 family: regulators of the cellular life-or-death switch. Nature Review Cancer 2, 647–656.

Davis, D.W., Buchholz, T.A., Hess, K.R., Sahin, A.A., Valero, V., McConkey, D.J., 2003. Automated quantification of apoptosis after neoadjuvant chemotherapy for breast cancer: early assessment predicts clinical response. Clinical Cancer Research 9, 955–960.

Hsieh, T.C., Wu, J.M., 2006. Differential control of growth, cell cycle progression, and gene expression in human estrogen receptor positive MCF-7 breast cancer cells by extracts derived from polysaccharopeptide I'm-Yunity and Danshen and their combination. International Journal of Oncology 29, 1215–1222.

Huang, H., Park, C.K., Ryu, J.Y., Chang, E.J., Lee, Y., Kang, S.S., Kim, H.H., 2006. Expression profiling of lipopolysaccharide target genes in RAW264.7 cells by oligonucleotide microarray analyses. Archives of Pharmacal Research 29, 890–897.

Hur, Y.G., Suh, C.H., Kim, S., Won, J., 2007. Rosmarinic acid induces apoptosis of activated T cells from rheumatoid arthritis patients via mitochondrial pathway. Journal of Clinical Immunology 27, 36–45.

Hur, Y.G., Yun, Y., Won, J., 2004. Rosmarinic acid induces $p56^{lck}$-dependent apoptosis in Jurkat and peripheral T cells via mitochondrial pathway independent from Fas/Fas ligand interaction. Journal of Immunology 172, 79–87.

Kang, J.X., Liu, J., Wang, J., He, C., Li, F.P., 2005. The extract of huanglian, a medicinal herb, induces cell growth arrest and apoptosis by up-regulation of interferon-β and TNF-α in human breast cancer cells. Carcinogenesis 26, 1934–1939.

Kang, T.H., Pae, H.O., Yoo, J.C., Kim, N.Y., Kim, Y.C., Ko, G.I., Chung, H.T., 2000. Antiproliferative effects of alkaloids from *Sedum sarmentosum* on murine and human hepatoma cell lines. Journal of Ethnopharmacology 70, 177–182.

Kawahata, T., Otake, T., Mori, H., Kojima, Y., Oishi, I., Oka, S., Fukumori, Y., Sano, K., 2002. A novel substance purified from *Perilla frutescens* Britton inhibits an early stage of HIV-1 replication without blocking viral adsorption. Antiviral Chemistry & Chemotherapy 13, 283–288.

Kim, D.S., Kim, H.R., Woo, E.R., Hong, S.T., Chae, H.J., Chae, S.W., 2005. Inhibitory effects of rosmarinic acid on adriamycin-induced apoptosis in H9c2 cardiac muscle cells by inhibiting reactive oxygen species and the activations of c-jun N-terminal kinase and extracellular signal-regulated kinase. Biochemical Pharmacology 70, 1066–1078.

Kolettas, E., Thomas, C., Leneti, E., Skoufos, I., Mbatsi, C., Sisoula, C., Manos, G., Evangelou, A., 2006. Rosmarinic acid failed to suppress hydrogen peroxide-mediated apoptosis but induced apoptosis of Jurkat cells which was suppressed by Bcl-2. Molecular and Cellular Biochemistry 285, 111–120.

Kuo, K.W., Hsu, S.H., Li, Y.P., Lin, W.L., Liu, L.F., Chang, L.C., Lin, C.C., Lin, C.N., Sheu, H.M., 2000. Anticancer activity evaluation of the solanum glycoalkaloid solamargine: triggering apoptosis in human hepatoma cells. Biochemical Pharmacology 60, 1865–1873.

Kyprianou, N., 2003. Doxazosin and terazosin suppress prostate growth by inducing apoptosis: clinical significance. Journal of Urology 169, 1520–1525.

Lee, J., Jung, E., Kim, Y., Lee, J., Park, J., Hong, S., Hyun, C.G., Park, D., Kim, Y.S., 2006. Rosmarinic acid as a downstream inhibitor of IKK-beta in TNF-alpha-induced upregulation of CCL11 and CCR3. British Journal of Pharmacology 148, 366–375.

Lee, S.P., Jun, G., Yoon, E.J., Park, S., Yang, C.H., 2001. Inhibitory effect of methyl caffeate on Fos-Jun-DNA complex formation and suppression of cancer cell growth. Bulletin of the Korean Chemical Society 22, 1131–1135.

Lim do, Y., Jeong, Y., Tyner, A.L., Park, J.H., 2007. Induction of cell cycle arrest and apoptosis in HT-29 human colon cancer cells by the dietary compound luteolin. American Journal of Physiology: Gastrointestinal and Liver Physiology 292, G66–G75.

Lin, C.S., Hsu, C.W., 2005. Differentially transcribed genes in skeletal muscle of Duroc and Taoyuan pigs. Journal of Animal Science 83, 2075–2086.

Luo, X., Budihardjo, I., Zou, H., Slaughter, C., Wang, X., 1998. Bid, a Bcl2 interacting protein, mediates cytochrome *c* release from mitochondria in response to activation of cell surface death receptors. Cell 94, 481–490.

Makino, T., Furuta, Y., Wakushima, H., Fujii, H., Saito, K., Kano, Y., 2003. Anti-allergic effect of *Perilla frutescens* and its active constituents. Phytotherapy Research 17, 240–243.

Osakabe, N., Yasuda, A., Natsume, M., Yoshikawa, T., 2004. Rosmarinic acid inhibits epidermal inflammatory responses: anticarcinogenic effect of *Perilla frutescens* extract in the murine two-stage skin model. Carcinogenesis 25, 549–557.

Peng, Y., Ye, J., Kong, J., 2005. Determination of phenolic compounds in *Perilla frutescens* L. by capillary electrophoresis with electrochemical detection. Journal of Agricultural and Food Chemistry 53, 8141–8147.

Salimei, P.S., Marfe, G., Di Renzo, L., Di Stefano, C., Giganti, M.G., Filomeni, G., Ciriolo, M.R., 2007. The interference of rosmarinic acid in the DNA fragmentation induced by osmotic shock. Frontiers in Bioscience 12, 1308–1317.

Selvendiran, K., Koga, H., Ueno, T., Yoshida, T., Maeyama, M., Torimura, T., Yano, H., Kojiro, M., Sata, M., 2006. Luteolin promotes degradation in signal transducer and activator of transcription 3 in human hepatoma cells: an implication for the antitumor potential of flavonoids. Cancer Research 66, 4826–4834.

Stennicke, H.R., Jurgensmeier, J.M., Shin, H., Deveraux, Q., Wolf, B.B., Yang, X., Zhou, Q., Ellerby, H.M., Ellerby, L.M., Bredesen, D., Green, D.R., Reed, J.C., Froelich, C.J., Salvesen, G.S., 1998. Pro-caspase-3 is a major physiologic target of caspase-8. Journal of Biological Chemistry 273, 27084–27090.

Takano, H., Osakabe, N., Sanbongi, C., Yanagisawa, R., Inoue, K., Yasuda, A., Natsume, M., Baba, S., Ichiishi, E., Yoshikawa, T., 2004. Extract of *Perilla frutescens* enriched for rosmarinic acid, a polyphenolic phytochemical, inhibits seasonal allergic rhinoconjunctivitis in humans. Experimental Biology and Medicine (Maywood) 229, 247–254.

Takeda, H., Tsuji, M., Matumiya, T., Kubo, M., 2002. Identification of rosmarinic acid as a novel antidepressive substance in the leaves of *Perilla frutescens* Britton var. acuta Kudo (*Perillae Herba*). Japanese Journal of Psychopharmacology 22, 15–22.

Ueda, H., Yamazaki, C., Yamazaki, M., 2002. Luteolin as an anti-inflammatory and anti-allergic constituent of *Perilla frutescens*. Biological & Pharmaceutical Bulletin 25, 1197–1202.

Ueda, H., Yamazaki, C., Yamazaki, M., 2003. Inhibitory effect of Perilla leaf extract and luteolin on mouse skin tumor promotion. Biological & Pharmaceutical Bulletin 26, 560–563.

Wang, Q.F., Chen, J.C., Hsieh, S.J., Cheng, C.C., Hsu, S.L., 2002. Regulation of Bcl-2 family molecules and activation of caspase cascade involved in gypenosides-induced apoptosis in human hepatoma cells. Cancer Letters 183, 169–178.

Yang, N.S., Shyur, L.F., Chen, C.H., Wang, S.Y., Tzeng, C.M., 2004. Medicinal herb extract and a single-compound drug confer similar complex pharmacogenomic activities in mcf-7 cells. Journal of Biomedical Science 11, 418–422.

Yoo, S.M., Oh, S.H., Lee, S.J., Lee, B.W., Ko, W.G., Moon, C.K., Lee, B.H., 2002. Inhibition of proliferation and induction of apoptosis by tetraandrine in HepG2 cells. Journal of Ethnopharmacology 81, 225–229.